Optical Engineering

SPIEDigitalLibrary.org/oe

Numerical study on wavelength-division multiplexing transmission of direct-detected amplitude and differential phase-shift keying-modulated signals using digital back-propagation

Sang-Gyu Park

Numerical study on wavelength-division multiplexing transmission of direct-detected amplitude and differential phase-shift keying-modulated signals using digital back-propagation

Sang-Gyu Park
Hanyang University
Department of Electronic Engineering
17 Haengdang-dong, Seongdong-gu
Seoul, 133–791, Korea
E-mail: sanggyu@hanyang.ac.kr

Abstract. This report is a detailed study on the application of digital back-propagation technique for wavelength-division multiplexing (WDM) transmission of amplitude and differential phase shift keying (ADPSK)-modulated signal. We find that the precompensation using digital back-propagation increases the transmission distance by more than a factor of two. We find that the performance improvement from digital precompensation strongly depends on the dispersion map of the transmission link and the optimum performance was obtained when about 3% to 5% of the span dispersion is under-compensated by in-line dispersion compensators and later compensated for at the end of the entire transmission link. We also find that the precompensation is robust enough to the variation of various link parameters which can occur in the deployment or operation of transmission systems.
[DOI: 10.1117/1.OE.51.2.025003]

Subject terms: digital back-propagation; precompensation; amplitude and differential phase-shift keying modulation; direct-detection; wavelength-division multiplexing optical transmission.

Paper 111076 received Sep. 4, 2011; revised manuscript received Nov. 7, 2011; accepted for publication Dec. 12, 2011; published online Mar. 7, 2012.

1 Introduction

Recently, various multi-level modulation formats have been investigated because of their superior spectral efficiency compared to binary formats.[1–6] Multi-level amplitude shift keying (ASK)[1] and multi-level differential phase shift keying (DPSK)[2,3] were the first multi-level formats tested in optical transmission. Since these formats use only one dimension in the signal space, it is difficult to increase the number of signal levels to more than 8 or 16. Therefore, modulation formats utilizing both the amplitude and phase space (or equivalently, the real and imaginary parts) of the signal are being investigated. The most famous example of them is quadrature amplitude modulation (QAM), in which both quadrature components of a signal are amplitude-modulated independently.[4–6]

QAM formats generally require coherent receivers to separate two quadrature components.[5] Although the realization of coherent receivers has become easier thanks to the advance of CMOS VLSI technology, still it would be very attractive if we could detect two-dimensional signals with direct-detection receivers. The amplitude and differential phase-shift keying (ADPSK) modulation format is a special class of QAM modulation format, in which symbols are arranged on concentric circles in the complex signal space so that (D)PSK and ASK parts of the signal can be detected independently.[7–9] The most important advantage of the ADPSK formats compared to conventional QAM formats is that they allow direct detection of both the phase and amplitude parts of the signal. Note that phase-modulated signals can be detected using one-bit-delayed Mach-Zhender interferometers (MZIs).

A fundamental challenge in the use of any multi-level modulation format is to secure adequate optical signal to noise ratio (OSNR). When the number of levels is increased, the OSNR required for a given target bit error rate (BER) increases. However, if we increase the signal power to satisfy the increased OSNR requirement, then the impairments from fiber nonlinearities degrade the system performance. The systems which use the ADPSK format with direct detection are especially vulnerable to the amplitude-symbol-dependent phase-shift due to self-phase modulation (SPM),[9] which severely degrades the DPSK-part performance. To overcome this difficulty, a number of remedies have been proposed. This author previously proposed a receiver with multiple delayed-arm interferometers of different relative phases between the arms.[10] Tran and Lowery proposed a scheme in which the SPM-induced phase rotation is precompensated at the transmitter.[11]

Recently, the nonlinearity compensation using digital back-propagation was proposed and demonstrated.[12–15] In this scheme, the signal distortion from fiber nonlinearities is compensated for by passing the signal through a digital system of which the characteristic is the reverse of the transmission link. The reverse transmission can be performed by numerically solving the well-known nonlinear Schrödinger equation.[16] Then, the predictable impairments from the fiber nonlinearities can be perfectly compensated for, and signal-optical noise and optical noise-optical noise interactions ultimately limit the system performance.

In this work, we numerically studied the application of digital back-propagation technique to wavelength-dimensional

0091-3286/2012/$25.00 © 2012 SPIE

multiplexing (WDM) transmissions of ADPSK-modulated signals using direct detection. In general, the back-propagation can be applied either as precompensation at the transmitter (TX) or as post-compensation at the receiver. However, since the employment of the back-propagation as post-compensation requires the use of coherent detection, it was used as precompensation in this work. We found that significant improvement in WDM as well as in single-channel transmission performance could be obtained by applying the back-propagation. The performance improvement strongly depended on the dispersion map of the transmission link. We also studied the sensitivity of the performance to the variation of various link parameters and found that the precompensation scheme tolerated the variation of parameters expected in the operation of real systems.

This paper is organized as follows: Section 2 describes the optical transmission system and the simulation setup used in this work. Section 3 details the performance of the precompensation in single-channel and WDM transmissions. Section 4 reports the sensitivity of the performance of the precompensated transmission on the link parameter variations.

2 System Description

In this work, we used a 32-level ADPSK modulation format with four amplitude levels and eight phase levels. Figure 1 shows the constellation diagram of the ADPSK format. The ratio of powers of different amplitude symbols was 1:2.47:4.56:7.26, which was identical to that used in Ref. 11. If we use a larger contrast ratio, then the performance of ASK-part improves at the expense of the DPSK-part performance, and vice versa. Whereas the true optimum ratio depends on the transmission distance and signal power, we have found that the system performance is not very sensitive to small variations of the ratio around the above value. The raw symbol rate was 24 Gbaud which corresponds to 120 Gbit/s of bit rate. This represents 20% of forward error correction (FEC) overhead when used for 100 Gbit/s transmissions.

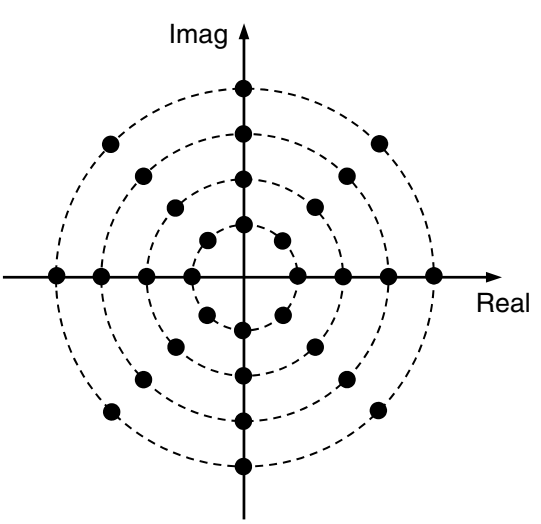

Fig. 1 Constellation diagram of the 32 level (4 amplitude levels × 8 phase levels) ADPSK modulation format used in this work.

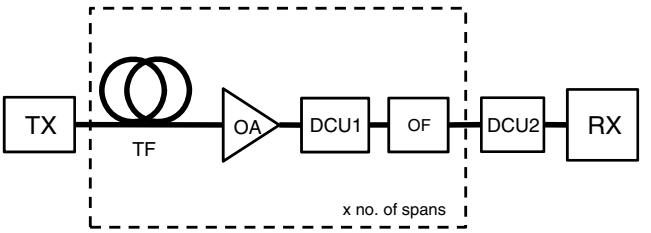

Fig. 2 Schematic diagram of the transmission system. TX: transmitter, RX: receiver, TF: transmission fiber, OA: optical amplifier, OF: optical filter, DCU1: in-line dispersion compensation unit, DCU2: dispersion compensation unit at the receiver site.

Figure 2 shows the schematic diagram of the transmission link studied in this work. The transmission fiber was the standard single-mode fiber (S-SMF), of which the loss, dispersion (D), dispersion slope ($\mathrm{dD/d\lambda}$), effective area and nonlinearity constant (n_2) were 0.25 dB/km, 17 ps/(nm · km), 0.07 ps/(nm^2 · km), 80 μm^2, and 2.6×10^{-8} μm$^2/W$, respectively. An amplifier span consists of 80 km of transmission fiber, an optical amplifier, an optical filter and a dispersion compensating unit (DCU). The gain and noise figure of the optical amplifier are 20 dB and 6 dB, respectively. The in-line optical filters, which have the bandwidth of 750 GHz, were used mainly to prevent aliasing back into the signal band of the high frequency optical noise generated by mixing of ASE components in the numerical simulation.

In this work, several dispersion maps were examined by changing the dispersion of the in-line DCU (DCU1) from −1360 ps/nm (100% in-line dispersion compensation) to 0 ps/nm (0% in-line dispersion compensation). When DCU1s did not completely compensate for the dispersion of the transmission fiber, an additional DCU was placed at the end of entire transmission link (DCU2) so that complete dispersion compensation was achieved. In this work, we focused on the ultimate performance limit of the digital back-propagation. Therefore, we assumed that the DCUs did not have any loss or nonlinearities and that the dispersion slope to dispersion ratio of the DCUs perfectly matched that of the transmission fiber.

Figure 3(a) shows the schematic of the transmitter. Using digital information to be transmitted as input, a digital precompensator generated ideal signal waveforms and digitally back-propagated them through a reverse transmission system. The ideal waveforms had carrier-suppressed return-to-zero (CS-RZ) pulse-shape with 67% of duty-ratio.[17] The electric field of the ADPSK modulated optical signal used in this work can be represented by Eq. (1),

$$e(t) = \sum_k A_k e^{j\varphi_k} \sin\left[\frac{\pi}{2}\cos\left(\frac{\pi t}{T_{sym}}\right)\right] u\left(\frac{t - \mathrm{kT_{sym}}}{T_{\mathrm{sym}}}\right), \tag{1}$$

where A_k, and φ_k are the amplitude and phase of the k-th symbol, T_{sym} is the symbol period and $u(t)$ is a unit pulse function defined as in Eq. (2).

$$u(t) = \begin{cases} 1, & |t| < 1/2 \\ 0, & \text{otherwise} \end{cases}. \tag{2}$$

In the reverse system, the order of elements and the sign of component parameters such as fiber loss parameter (α), fiber

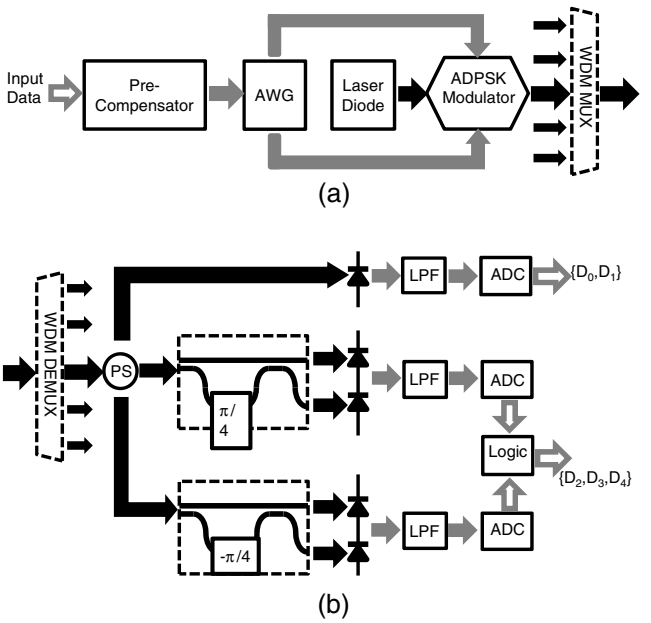

Fig. 3 Schematic diagram of (a) transmitter and (b) receiver. Black arrows: optical signal, grey arrows: electrical signal, hollow arrows: digital signal, PS: power splitter, AWG: arbitrary waveform generator, ADC: analog-to-digital converter.

nonlinearity parameter (n_2), fiber dispersion parameters (D and $dD/d\lambda$) and the gain of optical amplifiers (in dB) were reversed. The only exception to this was in-line optical filters, in that identical filters were used for both forward transmissions and back propagations. However, since the bandwidth of the optical filters used in this work was much broader than that of the signal, it had negligible effect. It should be noted that noiseless optical amplifiers were used in the back-propagation.

In a real transmission system, an arbitrary waveform generator (AWG) would receive the output of the precompensator in a (multi-bit) digital format and convert it into analog electrical waveforms, which drive an ADPSK modulator. The ADPSK modulator could be a dual drive MZI modulator biased at a null point for a linear transfer function. In this work, however, since numerical simulations were used for both forward transmission and back-propagation, no distinction was made between the outputs of precompensator, AWG, and ADPSK modulator, assuming that the nonlinear (sinusoidal) response of the MZI modulator could be compensated for digitally. The precompensated optical signals from multiple WDM channels were combined by a WDM multiplexer (MUX) and launched into the transmission link. The bandwidth of WDM MUX was optimized for each channel-spacing between 50 GHz to 70 GHz.

Figure 3(b) shows the configuration of the receiver. A WDM demultiplexer (DEMUX), which had the bandwidth of 30 GHz, selected the signal from the desired channel. The selected signal was then split into three parts and fed into an ASK receiver and two DPSK receivers. The ASK receiver consisted of a photo-diode, an electrical low-pass filter (LPF) of 24-GHz bandwidth and an analog-to-digital converter (ADC). The DPSK receivers have one-bit delayed MZIs, of which the relative phase between arms is $+\pi/4$ or $-\pi/4$. The output of an MZI was input to a pair of balanced photo-diodes, low-pass filtered and then digitized by an ADC. By combining the outputs of two ADCs of DPSK receivers using a simple logic circuit, the phase part of the transmitted information was recovered. In this work, the electrical noise generated by receivers was not considered, assuming that the optical amplifier noise dominated.

To simulate the signal propagation through fiber, we used a nonlinear Schrödinger equation solver based on the split-step Fourier method.[16] In the simulations, we used 2^{21} points to represent 2^{15} symbols. Therefore a symbol was represented by 2^6 points in the time domain. In the frequency domain, the free spectral range was $24\ \text{GHz} \times 2^6 = 1536\ \text{GHz}$. We used the same solver for forward and backward transmission simulations. In this work, BER was used as the measure of system performance. It was calculated by counting the number of errors after transmissions of 2^{15} symbols. With this number of symbols, a BER of 3×10^{-3} corresponds to 490 errors, which is large enough for statistical confidence. Note that with the FEC overhead of 20%, a raw BER of 3×10^{-3} can be converted to a BER of less than 1×10^{-15} after error correction.[18] Also note that we are assuming the use of a Gray coding so that a single symbol error leads to a single bit error most of the time.

3 Transmission Performance

3.1 *Single-Channel Transmissions*

As the first step, we performed simulations of single-channel transmissions with and without precompensation (i.e., back-propagation). Figure 4 shows the maximum transmission distance, which was defined as the distance by which BER grows to 3×10^{-3}, as a function of optical input power (P_{in}) into each span for each dispersion map. When the precompensation is not used (hollow symbols), the longest transmission distance was only 740 km and it was achieved with 100% in-line dispersion compensation at $P_{\text{in}} = 1$ dBm. When the nonlinear impairments were

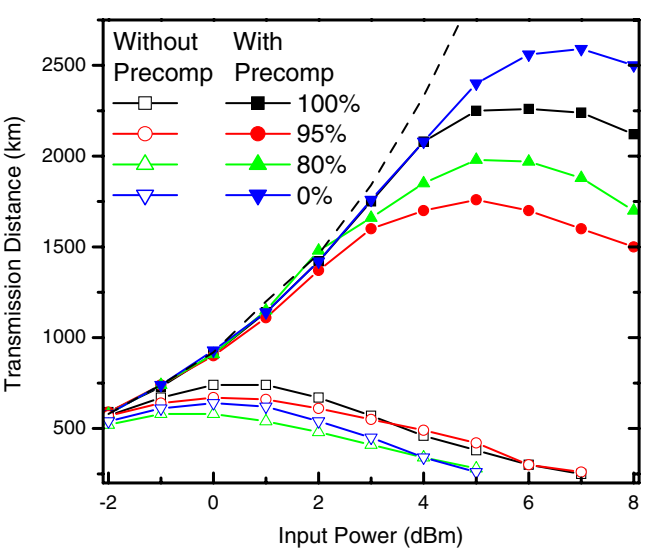

Fig. 4 BER performance of single-channel transmissions vs. input power to each span. with precompensation (solid symbols) and without precompensation (hollow symbols). Each type of symbol represents a different ratio of dispersion compensation by in-line DCU in each span. "100%" means complete in-line dispersion compensation, while "0%" means entire dispersion compensation at the end of the transmission link.

precompensated for by back-propagation (solid symbols), the transmission performance was greatly improved. The maximum transmission distance was extended to over 2500 km when 0% in-line dispersion compensation (i.e., 100% postcompensation) was used. The improvement was smaller when other dispersion maps were used. However, in all cases, the maximum distance exceeded 1700 km. Figure 4 also shows the OSNR-limited transmission distance, which was obtained by repeating the simulations without fiber nonlinearities ($n_2 = 0$). We can observe that when the precompensation is not used, the transmission distance begins to depart from the OSNR limit at $P_{in} = -1$ dBm. However, when the precompensation is used, the transmission distance remains close to the OSNR-limit even at $P_{in} = 2$ dBm due to the improved resilience against the nonlinear impairments.

3.2 *WDM Transmissions*

Next, we investigated the performance of the digital back-propagation in 5-channel WDM transmissions. Figure 5(a) shows the performance of the WDM transmission with precompensation. The channel spacing was 100 GHz. In this work, all WDM channels were co-polarized and no polarization related effects were considered. Figure 5(a) also shows the single-channel results already shown in Fig. 4. Figure 5(b) plots the maximum transmission distances of single-channel and WDM transmissions as functions of in-line dispersion compensation ratio. We observe that the performance improvement from the precompensation is reduced when applied to WDM transmissions. This is because our digital back-propagation does not compensate for the inter-channel nonlinear processes.[19] Nevertheless, when the link with 95% or 98% in-line dispersion compensation (i.e., 5% or 2% under-compensated spans) was used, transmission distances around 1600 km were obtained. That is very close to the maximum distance obtained in the single channel transmission from the same link, and more than one half of the best single-channel transmission distance obtained with 0% in-line dispersion compensation. In contrast, when the link with 0% in-line dispersion compensation is used in a WDM system, a transmission distance of less than 900 km was obtained, which was only one third of the single channel transmission distance obtained from that link.

Figure 6 compares the transmission distances obtained from different WDM channel spacings (Δf_{ch}). For Fig. 6, the link with 95% in-line dispersion compensation was used. At $\Delta f_{ch} = 50$ GHz, there is linear overlap between the spectra of neighboring channels, which causes a severe performance degradation. If we exclude this, we can observe that the maximum transmission distance decreases very slowly as the channel spacing is reduced. Even at $\Delta f_{ch} = 60$ GHz, a transmission distance of 1400 km was obtained. It is noted that the optimal input power decreased slightly from 5 to 4 dBm because the strength of the inter-channel nonlinearities grows as the channel spacing is reduced.

Up to this point, all WDM signals were constructed with an identical set of relative phases between WDM channels to maintain a consistency in the performance comparison. However, there can be some concerns regarding this. It can be suspected that different sets of relative phases

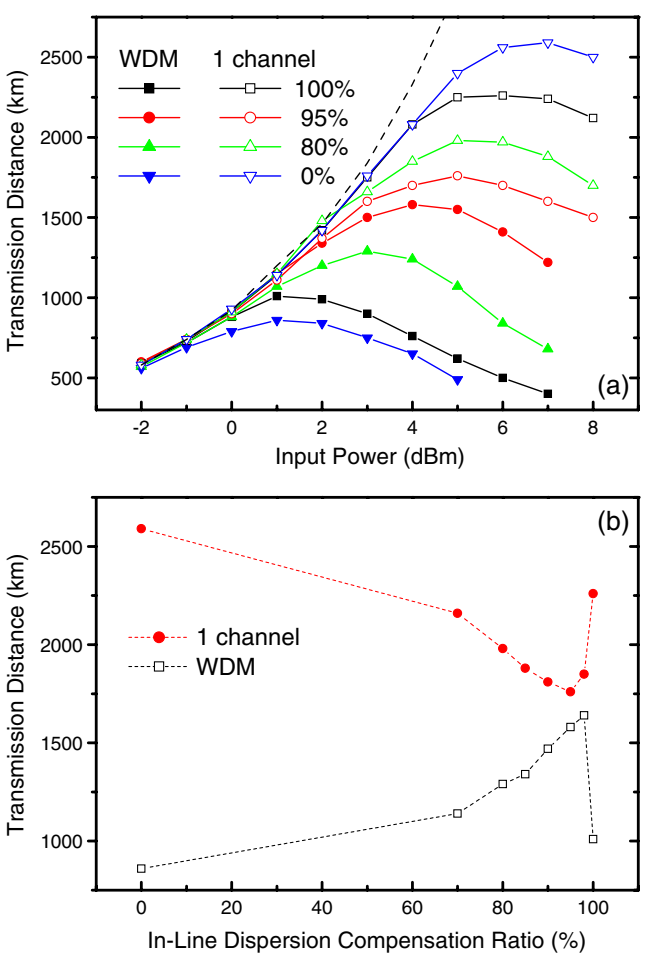

Fig. 5 (a) WDM (solid symbols) and single-channel (hollow symbols) transmission distances from the system using digital precompensation. In the case of WDM, five channels spaced at 100 GHz were used. The ratio of in-line dispersion compensation is indicated in the figure. (b) The maximum transmission distance obtained with the optimized power for each in-line dispersion compensation ratio.

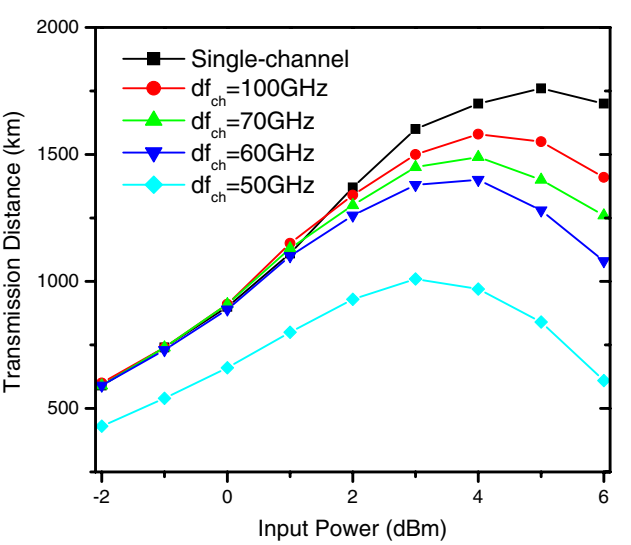

Fig. 6 Five-channel WDM transmissions with precompensation by digital back-propagation and 95% in-line dispersion compensation (i.e., 5% under-compensated spans.

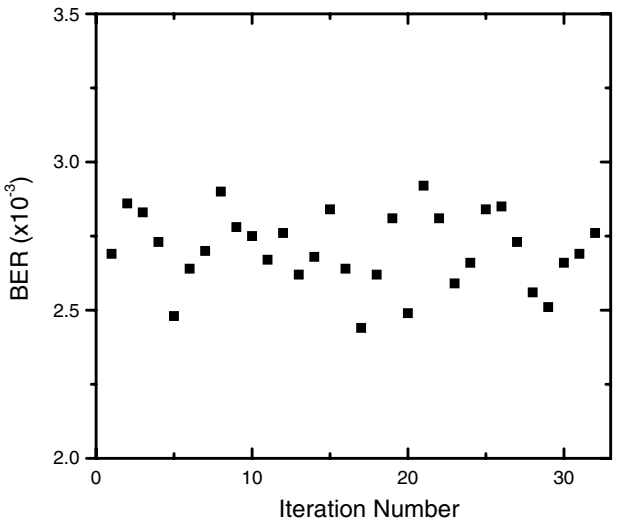

Fig. 7 The variation of BER when the relative phase and delay between channels are randomly varied (transmission distance 1360 km, P_{in} 4 dBm, channel spacing 60 GHz).

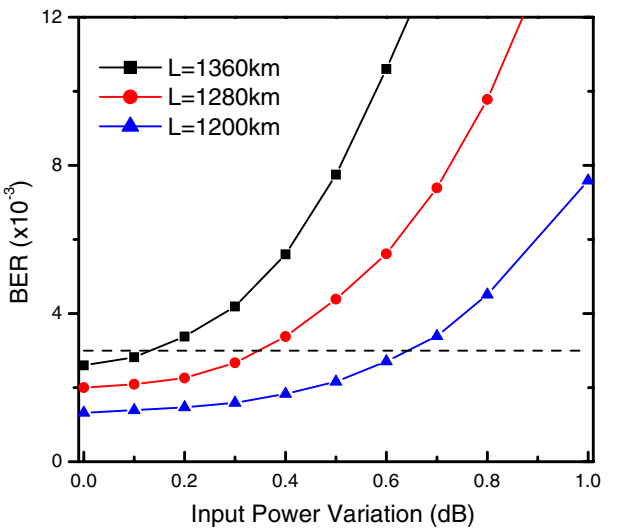

Fig. 8 BER degradation due to random fluctuations of optical input power to each span. The *x*-axis represents the standard deviation of the power variation in dB.

between channels might produce wildly different results. Then, our results from a single phase set might not be representative. To demonstrate that our results were indeed valid, we repeated our simulations with WDM signals constructed with different sets of relative phases between the channels. The results of the Monte-Carlo simulations with 32 iterations are shown in Fig. 7. The channel spacing, optical input power per channel, and the transmission distance were 60 GHz, 4 dBm and 1360 km, respectively. We observe that the BER varies by less than 20% between the maximum and the minimum. Thus, we can conclude with confidence that our results obtained with a single set of relative phase can properly represent the WDM system performance.

4 Sensitivity to the Link Parameter Variation

In a system deployed in the field, the values of parameters such as input power and fiber dispersion might be different from their nominal values. There might be inaccuracy involved with the installation or fluctuations due to temperature variations. Therefore, the sensitivity of the precompensation to the link parameter variation has to be addressed. First, transmission simulations were performed varying the input power to each span from the nominal value randomly according to Gaussian distribution. The simulations were performed using three precompensated signals, each of which were optimized for 1200 km, 1280 km or 1360 km of transmission distances, respectively. They all had WDM channel spacing of 60 GHz, and nominal input power of 4 dBm. Figure 8 shows the BER as a function of the standard deviation of the input power variation. We observe that the BER after 1360-km transmission rises from 2.6×10^{-3} to 3.0×10^{-3} when the variation of the input power grows to 0.12 dB. The BER after 1280-km or 1200-km transmission becomes larger than 3.0×10^{-3} when the variation exceeds 0.35 dB or 0.65 dB, respectively. Since the input power to spans can be controlled by optical amplifiers rather tightly, the input power variation is not expected to be a big issue in the implementation of digital back-propagation.

Next, we examined the BER degradation due to random variation of the chromatic dispersion of the transmission fiber. In this work, we assigned a random dispersion to each amplifier span and assumed that the dispersion was constant over the length of a span. Any residual accumulated dispersion of the entire transmission link was compensated for by the DCU at the receiver (DCU2) so that we did not simply measure the tolerance of the ADPSK modulation format against the linear impairment from the chromatic dispersion. Figure 9 shows the simulation results. The limits of the random deviation of fiber dispersion for BER $< 3 \times 10^{-3}$ are is 0.1 ps/(nm · km), 0.23 ps/(nm · km), or 0.41 ps/(nm · km) for 1360-km, 1280-km or 1200-km transmission, respectively. The chromatic dispersion of a fiber changes mainly due to temperature change and the temperature coefficient (TC) of the chromatic dispersion of most single mode fibers is smaller than 0.004 ps/(nm · km)/℃.[20] Therefore, even when the random temperature variation across the transmission link is as large as 100 ℃, the dispersion variation will not exceed 0.4 ps/(nm · km). Therefore, we expect

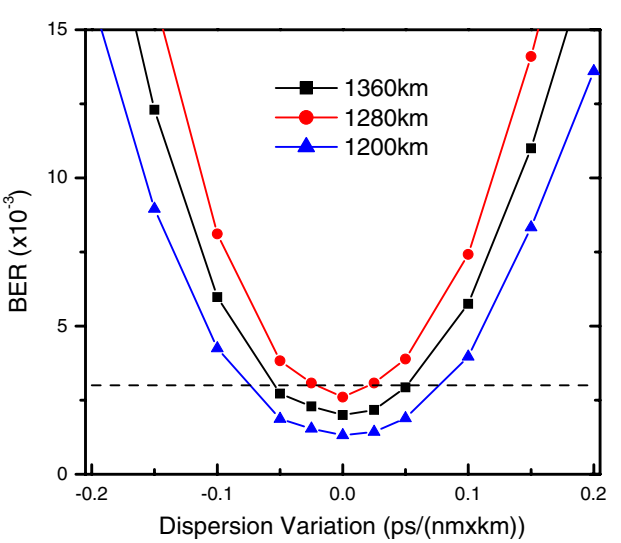

Fig. 9 BER degradation due to uniform drift of the fiber dispersion.

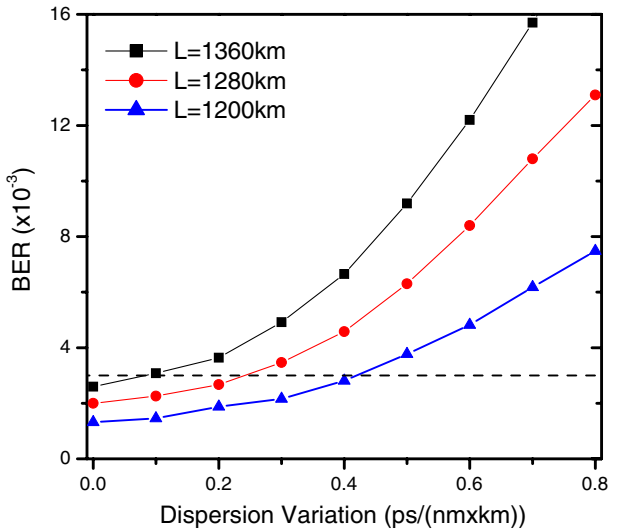

Fig. 10 BER degradation due to random variations of the fiber dispersion.

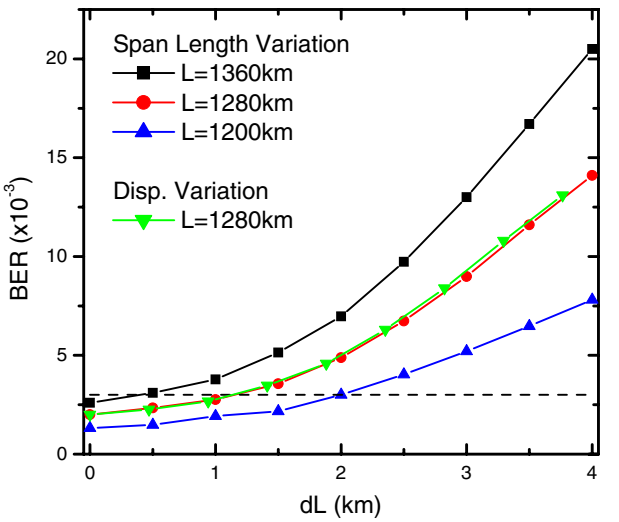

Fig. 11 Comparison of the BER degradations from span length variation (black, red, and blue symbols) and fiber dispersion variation (green inverted triangles). Input power to each span was kept constant at 4 dBm in both cases. For the dispersion variation case, the effective length variation defined in Eq. (3) is used as the x-axis.

that the random variation of fiber dispersion will not degrade the transmission performance significantly.

In the simulations of Fig. 10, the fiber dispersion fluctuated around the nominal value of 17 $\mathrm{ps}/(\mathrm{nm}\cdot\mathrm{km})$ so that the average remained unchanged. However, it is also possible that the average dispersion of the entire transmission fiber drifts from its nominal value. Figure 9 shows the simulation results for this case. Again, any residual dispersion was completely compensated for at the end of the link. We observe that the limit of the dispersion drift for BER BER $< 3\times10^{-3}$ is 0.025 $\mathrm{ps}/(\mathrm{nm}\cdot\mathrm{km})$, 0.05 $\mathrm{ps}/(\mathrm{nm}\cdot\mathrm{km})$ and 0.075 $\mathrm{ps}/(\mathrm{nm}\cdot\mathrm{km})$ for 1360 km, 1280 km or 1200 km of transmission length, respectively. For TC $= 0.004$ $\mathrm{ps}/(\mathrm{nm}\cdot\mathrm{km})/°C$, $\Delta D = 0.075$ $\mathrm{ps}/(\mathrm{nm}\cdot\mathrm{km})$ is translated into $\Delta T = 19°C$. This kind of temperature variation around a year is quite common. Therefore, if a fiber with such a large temperature coefficient is to be used, some measure, such as separate back-propagation for each temperature range, should be adopted. However, since this average temperature variation is a very slow process, and the relation between the temperature and the fiber dispersion is relatively well known, it is not expected to be a major problem.

Next, we examined the effect of random deviation of span length from the nominal value of 80 km. Figure 11 shows the BER as functions of the span length variation. The output power of the optical amplifiers was kept constant at 4 dBm despite the span loss variation associated with the length variation assuming that the optical amplifiers operated in fully saturated regime. The tolerable length variation was about 2 km for 1200-km transmissions. For 1360-km transmissions, it is reduced to 0.5 km, which is still an obtainable value.

When the length of a span is changed, it changes the span dispersion and span loss. However, if the span input power is kept constant by optical amplifiers in the saturated regime, then we can suppose that the main effect of the span length fluctuation is the fluctuation of the accumulated dispersion of fiber spans. To verify this, we compared the BER degradation from the span length fluctuation to that from fiber dispersion fluctuation for 1280-km transmissions. The empty triangles in Fig. 11 represent the degradation from dispersion variation, which were already presented in Fig. 10. Here, however, we used an effective length variation defined by Eq. (3):

$$\Delta L_{\mathrm{eff}} = (\Delta D/D_{\mathrm{TF}})L_{\mathrm{span}} \tag{3}$$

as the x-axis for the degradation from dispersion variation, where D_{TF}, and L_{span} are the chromatic dispersion of transmission fiber and the span length, respectively. This effective length represents the extra transmission fiber length to produce the same accumulated span dispersion fluctuation as the one produced by dispersion fluctuation. We can observe that the two curves for 1280-km transmissions are almost identical. This suggests that the variation of the fiber dispersion in a length scale smaller than the span length does not affect the performance significantly as long as the accumulated span dispersion remains the same, at least in the operating regime tested in this work.

5 Conclusions

In this paper, we studied the application of digital back-propagation technique to the transmission of ADPSK signal using direct detection. The performance of the ADPSK transmission was greatly improved by using digital back-propagation. It is very important that WDM as well as single-channel performance was improved by employing the digital back-propagation. In the absence of precompensation, the WDM transmission distance was limited to below 800 km even at channel spacing of 100 GHz. However, with the digital precompensation, the transmission distance was extended to 1700 km at 100-GHz spacing, and to 1400 km even at 60-GHz spacing. The performance of digital precompensation in WDM transmission strongly depends on the dispersion map of the transmission link. The optimum performance was obtained when about 5% of the span dispersion was under-compensated for by in-line dispersion compensators

and later compensated for at the end of the entire transmission link. To apply the precompensation technique in the field, it is important to verify that the performance is not too sensitive to the variations of the link parameters such as fiber dispersion and loss. We studied the sensitivity of the performance of the precompensation to the fluctuation of the link parameters and found that the precompensation was robust enough to provide the desired performance improvement in the field environment.

References

1. S. Walkin and J. Conradi, "Multilevel Signaling for Increasing the Reach of 10 Gb/s Lightwave Systems," *J. Lightwave Tech.* **17**(11), 2235–2248 (1999).
2. S. Chandrasekhar and X. Liu, "Experimental investigation of system impairments in polarization multiplexed 107-Gb/s RZ-DQPSK," in *Opt. Fiber Commun. Conf. (OFC)*, OSA Technical Digest (CD), Optical Society of America, paper OThU7 (2008).
3. M. S. Alfiad et al., "111-Gb/s POLMUX-RZ-DQPSK transmission over 1140 km of SSMF with 10.7-Gb/s NRZ-OOK neighbours," presented at *Euro. Opt. Commun. Conf. (ECOC) 2008*, Brussels, Belgium, paper Mo.4.E.2. (2008).
4. J. G. Proakis, *Digital Communications*, 3rd ed., McGraw-Hill, Boston, MA (1995).
5. M. Nakazawa et al., "256-QAM (64 Gb/s) coherent optical transmission over 160 km with an optical bandwidth of 5.4 GHz," *IEEE Photon. Technol. Lett.* **22**(3), 185–187 (2010).
6. H.-H. Lu and W.-J. Wang, "256-QAM WDM system transmitted over 80 km of single-mode fiber using a 1.3-μm semiconductor optical amplifier," *J. Opt. Eng.* **41**(11), 2707–2708 (2002).
7. S. Hayase et al., "Proposal of 8-state per symbol (binary ASK and QPSK) 30-Gbit/s optical modulation/demodulation scheme," presented at *Euro. Opt. Commun. Conf. (ECOC) 2003*, Rimini, Italy, paper Th2.6.4 (2003)
8. D. D. Tran, L. N. Binh, and T. L. Huynh, "Multi-level amplitude-differential phase shift keying (MADPSK) modulation formats for long-haul optical transmission systems," *Proc. SPIE* **635**(37), 1–11 (2006).
9. N. Kikuchi et al., "Study on cross-phase modulation (XPM) effect on amplitude and differentially phase-modulated multilevel signals in DWDM transmission," *IEEE Photon. Technol. Lett.* **17**(7), 1549–1551 (2005).
10. S.-G. Park, "APSK receiver for the cancellation of SPM-induced phase-shift," *IEEE Photon. Technol. Lett.* **18**(17), 1807–1809 (2006).
11. D. D. Tran and A. J. Lowery, "SPM mitigation in 16-ary amplitude-and-differential-phase shift keying long-haul optical transmission systems," *Opt. Express* **18**(8), 7790–7797 (2010).
12. R. I. Killey et al., "Electronic precompensation techniques to combat dispersion and nonlinearities in optical transmission," presented at *Euro. Opt. Commun. Conf.(ECOC) 2005*, Glasgow, UK, paper Tu4.2.1. (2005)
13. S. J. Savory, "Electronic signal processing in optical communications," *Proc. SPIE* **7136**, 71362C (2008).
14. K. Roberts et al., "Electronic precompensation of optical nonlinearity," *IEEE Photon. Technol. Lett.* **18**(2), 403–405 (2006).
15. E. M. Ip and J. M. Kahn, "Fiber impairment compensation using coherent detection and digital signal processing," *J. Lightwave Tech.* **28**(4), 502–519 (2010).
16. G. P. Agrawal, *Nonlinear Fiber Optics*, 3rd ed., Academic Press, San Diego, CA (2005).
17. Y. Miyamoto et al., "320 Gbit/s (8×40 Gb/s) WDM transmission over 367 km with 120 km repeater spacing using carrier-suppressed return-to-zero format," *Electron. Lett.* **35**(23), 2041–2042 (1999).
18. A. Tychopoulos, O. Koufopavlou, and I. Tomkos, "FEC in optical communications," *IEEE Circuits Dev.* **22**(6), 79–86 (Nov./Dec. 2006).
19. E. Mateo, L. Zhu, and G. Li, "Impact of XPM and FWM on the digital implementation of impairment compensation for WDM transmission using backward propagation," *Opt. Express* **16**(20), 16124–16137 (2008).
20. T. Kato, Y. Koyano, and M. Nishimura, "Temperature dependence of chromatic dispersion in various types of optical fiber," *Opt. Lett.* **25**(16), 1156–1158 (2000).

Sang-Gyu Park received BS and MS degrees in electronics engineering from Seoul National University in 1990 and 1992, respectively and received his PhD degree in electronic engineering from Purdue University in 1998. He worked at AT&T Laboratories-Research from 1998 to 2000 and joined the faculty of Hanyang University in 2000, where he is a professor in electronics and computer engineering. His research interests include optical transmission systems, optical CDMA networks, and semiconductor integrated circuits.